

## Article

# The Association of Gross Tumor Volume and Its Radiomics Features with Brain Metastases Development in Patients with Radically Treated Stage III Non-Small Cell Lung Cancer

Haiyan Zeng <sup>1,\*</sup>, Fariba Tohidinezhad <sup>1</sup>, Dirk K. M. De Ruyscher <sup>1</sup>, Yves C. P. Willems <sup>1</sup>, Juliette H. R. J. Degens <sup>2</sup>, Vivian E. M. van Kampen-van den Boogaart <sup>3</sup>, Cordula Pitz <sup>4</sup>, Francesco Cortiula <sup>1,5</sup>, Lloyd Brandts <sup>6</sup>, Lizza E. L. Hendriks <sup>7</sup> and Alberto Traverso <sup>1,8</sup>

<sup>1</sup> Department of Radiation Oncology (Maastr), GROW School for Oncology and Reproduction, Maastricht University Medical Centre+, 6229 ET Maastricht, The Netherlands; fariba.tohidinezhad@maastro.nl (F.T.); dirk.deruyscher@maastro.nl (D.K.M.D.R.); ycp.willems@student.maastrichtuniversity.nl (Y.C.P.W.); francesco.cortiula@maastro.nl (F.C.); alberto.traverso@maastro.nl or traverso.alberto@univr.it (A.T.)

<sup>2</sup> Department of Respiratory Medicine, Zuyderland Medical Center, 6419 PC Heerlen, The Netherlands; j.degens@zuyderland.nl

<sup>3</sup> Department of Pulmonology Diseases, VieCuri Medical Centre, 6200 MD Venlo, The Netherlands; vvankampen@viecuri.nl

<sup>4</sup> Department of Pulmonary Diseases, Laurentius Hospital, 6043 CV Roermond, The Netherlands; c.pitz@lzl.nl

<sup>5</sup> Department of Medical Oncology, University Hospital of Udine, 33100 Udine, Italy

<sup>6</sup> Department of Clinical Epidemiology and Medical Technology Assessment, Maastricht University Medical Center+, 6229 HX Maastricht, The Netherlands

<sup>7</sup> Department of Pulmonary Diseases, Maastricht, GROW School for Oncology and Reproduction, Maastricht University Medical Center+, 6202 AZ Maastricht, The Netherlands; lizza.hendriks@mumc.nl

<sup>8</sup> School of Medicine, Vita-Salute San Raffaele University, 20132 Milan, Italy

\* Correspondence: haiyan.zeng@maastro.nl or janezenghaiyan@outlook.com; Tel.: +31-88-44-55-600



**Citation:** Zeng, H.; Tohidinezhad, F.; De Ruyscher, D.K.M.; Willems, Y.C.P.; Degens, J.H.R.J.; van Kampen-van den Boogaart, V.E.M.; Pitz, C.; Cortiula, F.; Brandts, L.; Hendriks, L.E.L.; et al. The Association of Gross Tumor Volume and Its Radiomics Features with Brain Metastases Development in Patients with Radically Treated Stage III Non-Small Cell Lung Cancer. *Cancers* **2023**, *15*, 3010. <https://doi.org/10.3390/cancers15113010>

Academic Editors: Lisa Deloch, Johann Matschke, Michael Rückert and David Wong

Received: 10 May 2023  
Revised: 22 May 2023  
Accepted: 26 May 2023  
Published: 31 May 2023



**Copyright:** © 2023 by the authors. Licensee MDPI, Basel, Switzerland. This article is an open access article distributed under the terms and conditions of the Creative Commons Attribution (CC BY) license (<https://creativecommons.org/licenses/by/4.0/>).

**Simple Summary:** Around 30% of patients with stage III non-small cell lung cancer (NSCLC) receiving radical chemoradiotherapy will develop symptomatic brain metastases (BM) during the disease course. Identifying risk factors for BM can help improve the management of these patients. The aim of this current study was to identify clinical risk factors, including gross tumor volume (GTV) radiomics features, for developing BM in patients with radically treated stage III NSCLC. We found that age, NSCLC subtype, and GTV of lymph nodes (GTVn) were significant factors for BM. GTVn radiomics features provided higher predictive value than GTV of primary tumor (GTVp) and GTV. Therefore, GTVp and GTVn should be separated in clinical and research practice.

**Abstract:** Purpose: To identify clinical risk factors, including gross tumor volume (GTV) and radiomics features, for developing brain metastases (BM) in patients with radically treated stage III non-small cell lung cancer (NSCLC). Methods: Clinical data and planning CT scans for thoracic radiotherapy were retrieved from patients with radically treated stage III NSCLC. Radiomics features were extracted from the GTV, primary lung tumor (GTVp), and involved lymph nodes (GTVn), separately. Competing risk analysis was used to develop models (clinical, radiomics, and combined model). LASSO regression was performed to select radiomics features and train models. Area under the receiver operating characteristic curves (AUC-ROC) and calibration were performed to assess the models' performance. Results: Three-hundred-ten patients were eligible and 52 (16.8%) developed BM. Three clinical variables (age, NSCLC subtype, and GTVn) and five radiomics features from each radiomics model were significantly associated with BM. Radiomic features measuring tumor heterogeneity were the most relevant. The AUCs and calibration curves of the models showed that the GTVn radiomics model had the best performance (AUC: 0.74; 95% CI: 0.71–0.86; sensitivity: 84%; specificity: 61%; positive predictive value [PPV]: 29%; negative predictive value [NPV]: 95%; accuracy: 65%). Conclusion: Age, NSCLC subtype, and GTVn were significant risk factors for BM. GTVn radiomics features provided higher predictive value than GTVp and GTV for BM development. GTVp and GTVn should be separated in clinical and research practice.

**Keywords:** non-small cell lung cancer (NSCLC); brain metastases (BM); gross tumor volume (GTV); radiomics; thoracic radiotherapy

## 1. Introduction

Up to 30% of patients with stage III non-small cell lung cancer (NSCLC) receiving radical chemoradiotherapy will develop symptomatic brain metastases (BM) during the course of their disease [1]. Identifying risk factors for BM can help improve the management of these patients. Known risk factors are female sex, adenocarcinoma or non-squamous cell carcinoma histology, and advanced tumor stage [2–4]. Whether a higher gross tumor volume (GTV) is a risk factor for subsequent BM development remains unclear. It has been reported that GTV is a prognostic factor for locoregional control [5], progression-free survival (PFS) [6], and OS [6–9] in patients with NSCLC. Ji et al. found that GTV is not a significant risk factor for BM in patients with NSCLC ( $n = 335$ ,  $p = 0.687$ ) [10], whereas a larger GTV was associated with an increased risk of BM in patients with small-cell lung cancer (SCLC) (HR = 1.37, 95% CI 1.09–1.73,  $p = 0.007$ ) [11].

Radiomics is increasingly being used in cancer risk prediction [12,13] and is, based on the seed-and-soil hypothesis, also of interest to evaluate in stage III NSCLC (primary tumor and/or involved lymph nodes) and in the BM prediction setting [14]. It is a quantitative imaging analysis technique that provides image-derived metrics capable of quantifying textures at a higher granularity, beyond the ability of the naked eye. Four studies showed that radiomic models based on pretreatment computed tomography (CT) might predict BM in NSCLC, but the models did not always add value to clinical models [15–19]. Important limitations of these studies were small sample sizes, inadequate baseline staging, only evaluating the primary tumor and not the involved lymph nodes, and the use of heterogeneous CT protocols. Thus, it is difficult to draw firm conclusions.

According to the backgrounds and rationales above, we conducted the current study to explore risk factors and develop prognostic models for BM in radically treated stage III NSCLC. We used a large dataset with adequately staged patients (baseline  $^{18}\text{F}$ -labeled fluorodeoxyglucose positron emission tomography–CT scan [ $^{18}\text{F}$ FDG-PET-CT] and brain magnetic resonance imaging [MRI]) and evaluated clinical data together with radiomics features of GTVs on the uniformly scanned planning contrast-enhanced chest CT for thoracic radiotherapy.

## 2. Patients and Methods

Patients with stage III NSCLC were retrospectively screened in five hospitals in the Netherlands and Italy (MUMC, Zuyderland, Venlo, Roermond, Udine) from 1 March 2012 to 31 July 2021. AJCC 7th edition was used for staging [20]. Eligibility criteria for this study included pathologically confirmed NSCLC,  $^{18}\text{F}$ FDG-PET-CT and brain MRI performed at baseline (before antitumor therapy), treatment with chemoradiotherapy with radical intent (concurrent or sequential chemoradiotherapy, CCRT/SCRT). Exclusion criteria were participation in interventional clinical trials (NVALT-11 trial [because of prophylactic cranial irradiation [PCI] administration in one arm] [1], PET-boost trial [because of radiotherapy dose-escalation] [21], and NICOLAS trial [because of nivolumab] [22]), other malignancy within 5 years before NSCLC diagnosis; surgery for NSCLC before chemoradiotherapy, and a total irradiation dose (TD) < 54Gy. Proton therapy, all types of platinum doublet chemotherapy, and adjuvant durvalumab were allowed. This study was conducted in accordance with the Helsinki Declaration of the World Medical Association and approved by the institutional review boards (W 22 01 00010). Informed consent from individuals for the use of their medical data was waived because no additional interventions were performed.

### 2.1. Acquisition of Images

The original planning CTs were retrieved from the clinical workstation database. All the images were acquired with contrast enhancement and with a slice thickness of 3 mm with consistent acquisition parameters on the two scanner manufacturers (Philips or SIEMENS). The pixel spacing varied from a minimum of 0.976 mm to a maximum of 1.52 mm in the X and Y directions.

### 2.2. Delineation of Regions of Interest (ROI)/GTV

The ROIs were the original GTVs obtained from the planning CT scan. The GTVs were delineated by a team of specialists in lung cancer radiotherapy in each slice of the planning CT based on the most recent  $^{18}\text{F}$ FDG-PET information using the ARIA workstation (Varian, Palo Alto, CA, USA). GTV of the primary tumor (GTVp) and lymph nodes (GTVn) were delineated separately if anatomically distinguishable. When it was difficult to distinguish the primary tumor or lymph nodes, the tumor was contoured as either GTVp or GTVn (the choice was left to experienced radiation oncologist). GTV was calculated as the morphological union of GTVp and GTVn. The lung window setting ( $W = 200$  HU and  $L = -1000$  HU [Hounsfield Units]) was used to contour tumors surrounded by lung tissue and the mediastinum window setting ( $W = 220$  HU and  $L = -180$  HU) was applied for the contouring of lymph nodes and primary tumors invading the mediastinum or chest wall [23]. The contouring of each patient was confirmed by a senior radiation oncologist (experience >10 years).

### 2.3. GTV Radiomics Features Extraction

The pipeline for radiomic feature extraction consisted of the following steps: data conversion and pre-processing, radiomic extraction configuration and feature extraction. The data conversion was performed using an in-house Python script that converts the original DICOM and RTSTRUCT images into the .nrrd format that is mineable by pyradiomics. The Python packages simpleITK v2.1 and pyplasticmatch v1.9.3 were used to convert the original DICOM CT images and the contours GTV, GTVp, GTVn into .nrrd images and corresponding binary masks. The radiomic extraction configuration included the following operations: re-sampling of the original images to the same pixel spacing of [1,1,1] using B-spline interpolation, removal of outliers from the binary masks above  $3\sigma$  from the distribution of intensity values for each patient, application of wavelet filtering in all the 13 directions to generate wavelet features. The following feature categories were extracted from both original and wavelet-filtered images: first-order statistical features, and texture feature matrixes (GLCM, GLSZM, GLRLM, NGTDM). Morphological features were extracted only from the original images. The fixed-bin width approach ( $n = 25$ ) was chosen for the quantization of statistical and texture features. The details of the source code are published on a public repository (<https://github.com/Maastro-CDS-Imaging-Group/GTVNSCLC>; accessed on 27 March 2023). The features were normalized to Z-score, as is common practice in statistical analyses.

### 2.4. Clinical and Treatment-Related Variables

In addition to GTV, other potential factors for BM were also recorded and investigated, including age, sex, smoking history, body mass index (BMI), performance status (PS), histology type, TNM stage at diagnosis; chemoradiotherapy type (concurrent or sequential chemoradiotherapy, CCRT/SCRT), total dose of radiotherapy, type of radiotherapy (once-daily radiotherapy, ODRT; twice-daily radiotherapy, TDRT/mix [TDRT + ODRT]), and immunotherapy.

### 2.5. Statistics

Missing data of the clinical variables were imputed by multiple imputation. Then, GTV, GTVn, and GTVp were divided into three categories by interquartile range (IQR) for risk analysis. The primary endpoint was BM confirmed by cranial imaging at any time

regardless of presence of neurologic symptoms (e.g., headache or vomiting). The secondary endpoints were PFS (progression of disease at the first time in any sites confirmed by imaging or death) and OS. All endpoints were analyzed as time-to-event data from the pathological diagnosis to the respective events, which were subject to censoring at the last follow-up if no events were observed. The BM was analyzed using competing risk analysis, in which death without BM was treated as a competing event. The significant clinical risk factors (including volume of GTVs, which was excluded from the radiomic features analysis) for BM were identified using the multivariate Fine-Gray model with backward stepwise elimination [24,25].

Radiomic feature selection was performed using 1000 bootstrap resamples [26–28]. Within each of the 1000 bootstrap resamples, Spearman’s correlation was performed to identify and eliminate the highly correlated features ( $|r| > 0.9$ ). Then, the least absolute shrinkage and selection operator (LASSO) embedded with the Fine-Gray model was used to select features ( $\lambda = 0.01$ ). The features were sorted according to how frequently they were retained by LASSO in 1000 bootstrap resamples. We arbitrarily selected the top 13 features as the input for the backward stepwise competing risk model on the same 1000 bootstrap resamples. Then, we arbitrarily selected the top signature (more than one radiomic feature) to build the radiomic models. The coefficients were fitted using the original sample. A maximum number of five predictors was considered for each model to reduce the risk of overfitting. To build the combined model, one feature with the highest effect estimate (according to subdistribution hazard ratio [sHR]) from each model (Clinic + GTV + GTVp + GTVn) was selected.

The performance of competing-risk models at the 24 months’ time point was evaluated by area under the receiver operating characteristic curves (AUC-ROC) and calibration. The sensitivity, specificity, negative predictive value (NPV), positive predictive value (PPV), and accuracy of each model were also reported. The net-benefit decision-curve analysis (DCA) was performed to compare the models’ utility/application value [26]. A nomogram would be developed for the clinical model. If the radiomics model or combined model performed better, a nomogram would also be developed for the best one [28] (Figure 2.5). The time point of 24 months was chosen because most of BM develop within 2 years [1]. The effect of significant BM risk factors (features) on PFS and OS were investigated by Cox proportional hazards regression models. All tests were 2-sided, and  $p < 0.05$  were considered as statistically significant. Statistical analyses were performed using R version 4.2.2 (R Project for Statistical Computing).

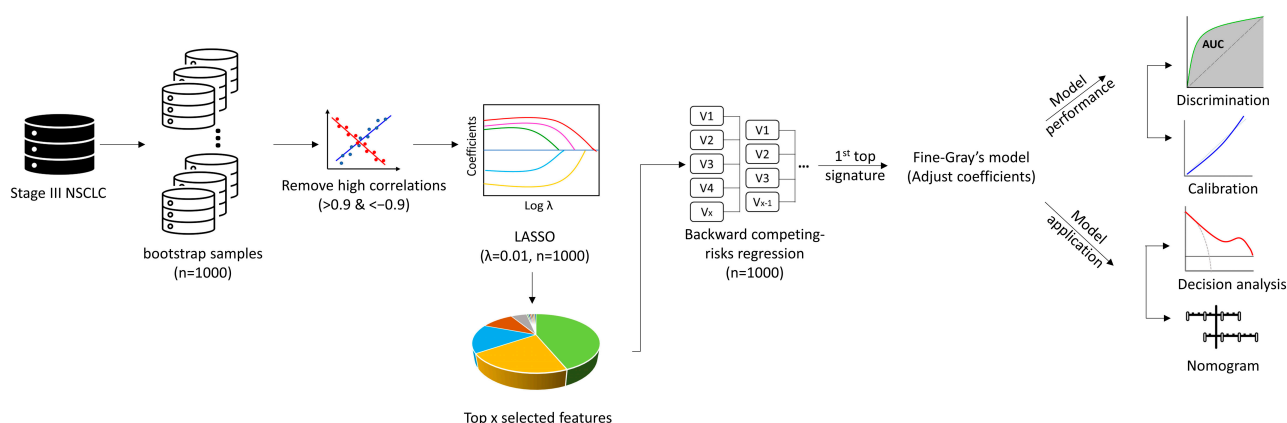


**Figure 1.** Analysis pipeline of radiomics models. This figure shows the analysis pipeline for development and evaluation of the radiomics prediction models: I, resample by 1000 bootstrap; II, eliminate highly correlated features; III, select features by LASSO regression embedded with the Fine–Gray model; IV, select top features retained by LASSO in 1000 bootstrap resamples; V, evaluate the features’

associations with BM using backward stepwise competing risk model; VI, select the top signatures to build the radiomic models using the original sample; VII, evaluate the performance of the models by AUC and calibration curve; VIII, evaluate the utility of the models by the net–benefit decision–curve analysis; IX, develop a nomogram for the best model. *Abbreviations:* AUC, area under the receiver operating characteristic curves; LASSO, least absolute shrinkage and selection operator; NSCLC, non-small cell lung cancer.

This type 2A study was conducted according to the Transparent Reporting of a multi-variable prediction model for Individual Prognosis Or Diagnosis (TRIPOD) guideline [29]. The TRIPOD checklist was reported in Appendix A Table A1.

### 3. Results

In total, 310 out of 524 patients were eligible, 282 of the 310 patients had available DICOM images for radiomic analysis (260 had GTVp, 254 had GTVn, 231 had GTVp + GTVn) (CONSORT diagram in Figure 2). Twenty-one patients had indistinguishable GTVp/GTVn, of which 12 were contoured as GTVn, nine as GTVp. Among the 310 patients, 54.5% were male, 51.6% had stage IIIA, and 37.4% had squamous-cell carcinoma (SCC), the median GTV was 71.2 (IQR: 35.2–115.2) cm<sup>3</sup>, the median GTVn was 16.4 (IQR: 0.88–244.1) cm<sup>3</sup> and the median GTVp was 41.4 (IQR: 9.8–89) cm<sup>3</sup> (Table 1). The median follow-up was 51.3 months (95% CI: 42.9–59.7 months), during which 176 (56.8%) patients died, 183 (59.0%) progressed, and 52 (16.8%) developed BM. The median OS was 34.8 months (95% CI: 28.4–41.2 months) and the median PFS was 19.3 months (95% CI: 15.1–23.5 months). For the 52 patients who developed BM, the median time to BM diagnosis was 10.5 months (95% CI: 9.2–11.9 months), the BM incidence at 2 years was 14.5%.

**Table 1.** Patients characteristics (*n* = 310).

Characteristics	Number (%)
Age	
Mean ± SD	65.7 ± 8.4
≤60	80 (25.8)
>60	230 (74.2)
Male gender	169 (54.5)
Body mass index-kg/m <sup>2</sup>	
Normal (18.5–24.9)	137 (44.2)
Underweight (<18.5)	13 (4.2)
Overweight (25.0–29.9)	113 (36.5)
Obese (≥30)	47 (15.2)
Smoking	
Never/Former	174 (56.1)
Current	136 (43.9)
Performance status	
0	123 (39.7)
1	160 (51.6)
2–3	27 (8.7)
TNM_T	
0/X/1/2/3	171 (55.2)
4	139 (44.8)
TNM_N	
0–1	38 (12.3)
2	210 (67.7)
3	62 (20.0)
Stage	
IIIA	160 (51.6)
IIIB	150 (48.4)

**Table 1.** *Cont.*

Characteristics	Number (%)
Histology	
Squamous-cell	116 (37.4)
Non-Squamous-cell	194 (62.6)
Chemoradiotherapy	
Concurrent	277 (89.4)
Sequential	33 (10.6)
Type of radiation	
OD	205 (66.1)
TD/TD+OD	105 (33.9)
Total dose (Gy)	
≤66	226 (72.9)
>66	84 (27.1)
Adjuvant immunotherapy	84 (27.1)
GTV (cm <sup>3</sup> )	
Median (range)	71.2 (4.3–1252.8)
<35.2	78 (25.2)
35.2–115.2	153 (49.4)
>115.2	79 (25.5)
GTVn (cm <sup>3</sup> )	
Median (range)	16.4 (0–244.1)
<6	78 (25.2)
6–36.4	154 (49.7)
>36.4	78 (25.2)
GTVp (cm <sup>3</sup> )	
Median (range)	41.4 (0–1195.6)
<9.8	78 (25.2)
9.8–89	154 (49.7)
>89	78 (25.2)

*Abbreviations:* GTV, gross tumor volume; GTVp, gross tumor volume-primary lung tumor; GTVn, gross tumor volume-metastatic lymph nodes; SD, standard deviation.

### 3.1. BM Risk Models

The clinical model identified three significant factors associated with BM: a higher age (>60 years) was protective (sHR 0.56, 95% CI 0.32–0.99,  $p = 0.05$ ), while non-squamous histology (sHR 2.64, 95% CI 1.28–5.46,  $p = 0.009$ ), and a larger GTVn (median IQR: sHR 3.76, 95% CI 1.33–10.61,  $p = 0.012$ ; upper IQR: sHR 3.86, 95% CI 1.28–11.65,  $p = 0.017$ ) were associated with an increased risk. GTV, GTVp, the use of adjuvant durvalumab, and other clinical variables were not significantly associated with BM development (Table 2).

We extracted 861 radiomic features in total and identified five GTV features, five GTVn features, and five GTVp features that were associated with BM (Table 2). The combined model of the first top feature from each model showed that the GTVn radiomics feature (LLH glrlm Run Variance: sHR 1.53, 95% CI 1.05–2.24,  $p = 0.028$ ) and the GTVp radiomics feature (HLH glszm Grey Level Non Uniformity: sHR 1.52, 95% CI 1.29–1.79,  $p < 0.001$ ) were significantly associated with an increased risk of BM development, while the clinical variable (volume of GTVn) and GTV radiomics feature were not (Table 2).

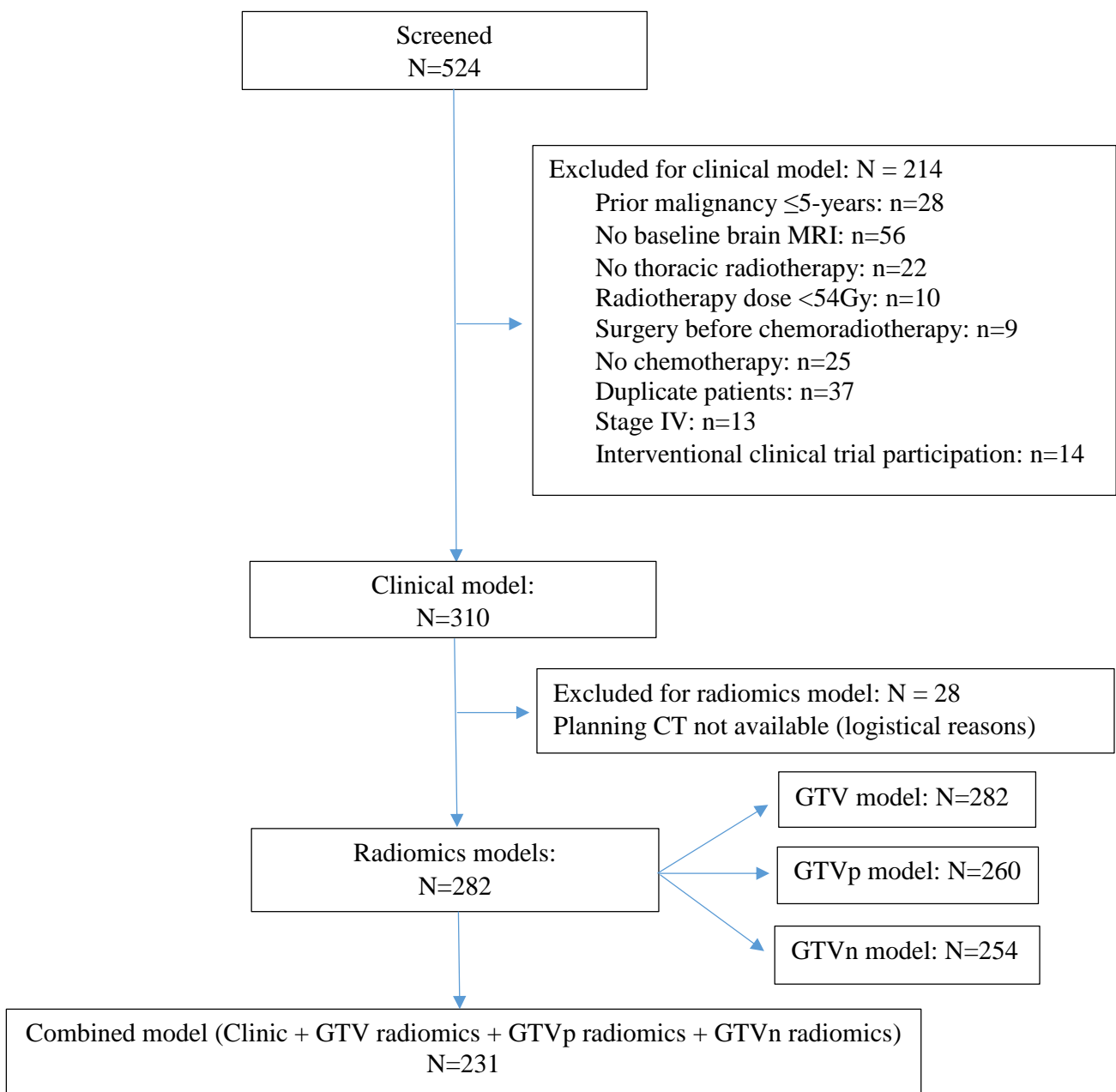


**Figure 2.** CONSORT diagram. This diagram shows the patients screening and available sample size for each model. *Abbreviations:* CT, computed tomography; GTV, gross tumor volume; GTVp, GTV of the primary tumor; GTVn, GTV of the involved lymph nodes; MRI, magnetic resonance imaging.

**Table 2.** BM competing risk models.

	sHR	95% CI	p
<b>Clinical model</b> ( <i>n</i> = 310, 52 BM)			
Age (>60 vs. ≤60)	0.56	0.32–0.99	<b>0.045</b>
Histology (Non-Squamous vs squamous)	2.64	1.28–5.46	<b>0.009</b>
GTVn (cm <sup>3</sup> )			
<6		[Reference]	
6–36.4	3.76	1.33–10.61	<b>0.012</b>
>36.4	3.86	1.28–11.65	<b>0.017</b>
<b>GTV radiomic model</b> ( <i>n</i> = 282, 46 BM)			
HLH firstorder Median	0.63	0.50–0.78	<b>&lt;0.001</b>
HLH glcm Imc1	1.72	1.13–2.61	<b>0.011</b>
Original firstorder Skewness	1.39	1.17–1.64	<b>&lt;0.001</b>
Original glszm Zone Entropy	0.66	0.50–0.87	<b>0.003</b>
HHH glszm Small Area Emphasis	1.66	1.17–2.35	<b>0.004</b>
<b>GTVn radiomic model</b> ( <i>n</i> = 254, 44 BM)			
LLH glrlm Run Variance	1.77	1.26–2.48	<b>0.001</b>
HLH glcm Imc1	1.67	1.14–2.46	<b>0.009</b>
HLH glszm Small Area Low Grey Level Emphasis	0.58	0.38–0.89	<b>0.012</b>
LLH glszm Size Zone Non Uniformity Normalized	1.54	1.27–1.87	<b>&lt;0.001</b>
HHL glszm Grey Level Non Uniformity Normalized	0.67	0.48–0.93	<b>0.018</b>
<b>GTVp radiomic model</b> ( <i>n</i> = 260, 39 BM)			
LHH glszm Small Area Low Grey Level Emphasis	1.66	1.29–2.14	<b>&lt;0.001</b>
LLH glcm Cluster Shade	1.40	1.10–1.80	<b>0.007</b>
HLH glszm Grey Level Non Uniformity	1.90	1.58–2.29	<b>&lt;0.001</b>
HLL firstorder Root Mean Squared	0.62	0.43–0.90	<b>0.013</b>
LLL glcm Imc1	1.93	1.06–3.51	<b>0.032</b>
<b>Combined model</b> ( <i>n</i> = 231, 37 BM)			
GTVn (cm <sup>3</sup> )			
<6		[Reference]	
6–36.4	3.09	0.68–13.98	0.143
>36.4	2.49	0.50–12.53	0.268
GTV HLH glcm Imc1	1.33	0.82–2.16	0.242
GTVn LLH glrlm Run Variance	1.53	1.05–2.24	<b>0.028</b>
GTVp HLH glszm Grey Level Non Uniformity	1.52	1.29–1.79	<b>&lt;0.001</b>

Abbreviations: BM, brain metastases; CI, confidence interval; GTV, gross tumor volume; GTVp, gross tumor volume-primary lung tumor; GTVn, gross tumor volume-metastatic lymph nodes; sHR, subdistribution hazard ratio.

### 3.2. Evaluation of the Models' Performance

The AUCs at each time point showed that the GTVn radiomics model performed best to discriminate the patients that did and did not develop BM (AUC range: 0.71–0.74) (Figure 3A).

At 24 months, the GTVn radiomics model had the highest AUC (0.74, 95% CI: 0.71–0.86), sensitivity (84%), and the NPV (95%); the GTVp radiomics model has the highest specificity (80%), PPV (34%), and accuracy (76%) (Table 3). The calibration plot also visually showed that the GTVn radiomic model had the best calibration within 24 months (Figure 3B). The decision curve analysis showed that compared with the other models, the GTVn radiomic model provided a better net benefit for the threshold probabilities smaller than 0.3 (Figure 3C). Therefore, a nomogram was developed for the clinical model (Figure 3D) and the GTVn radiomics model (Figure 3E), respectively.

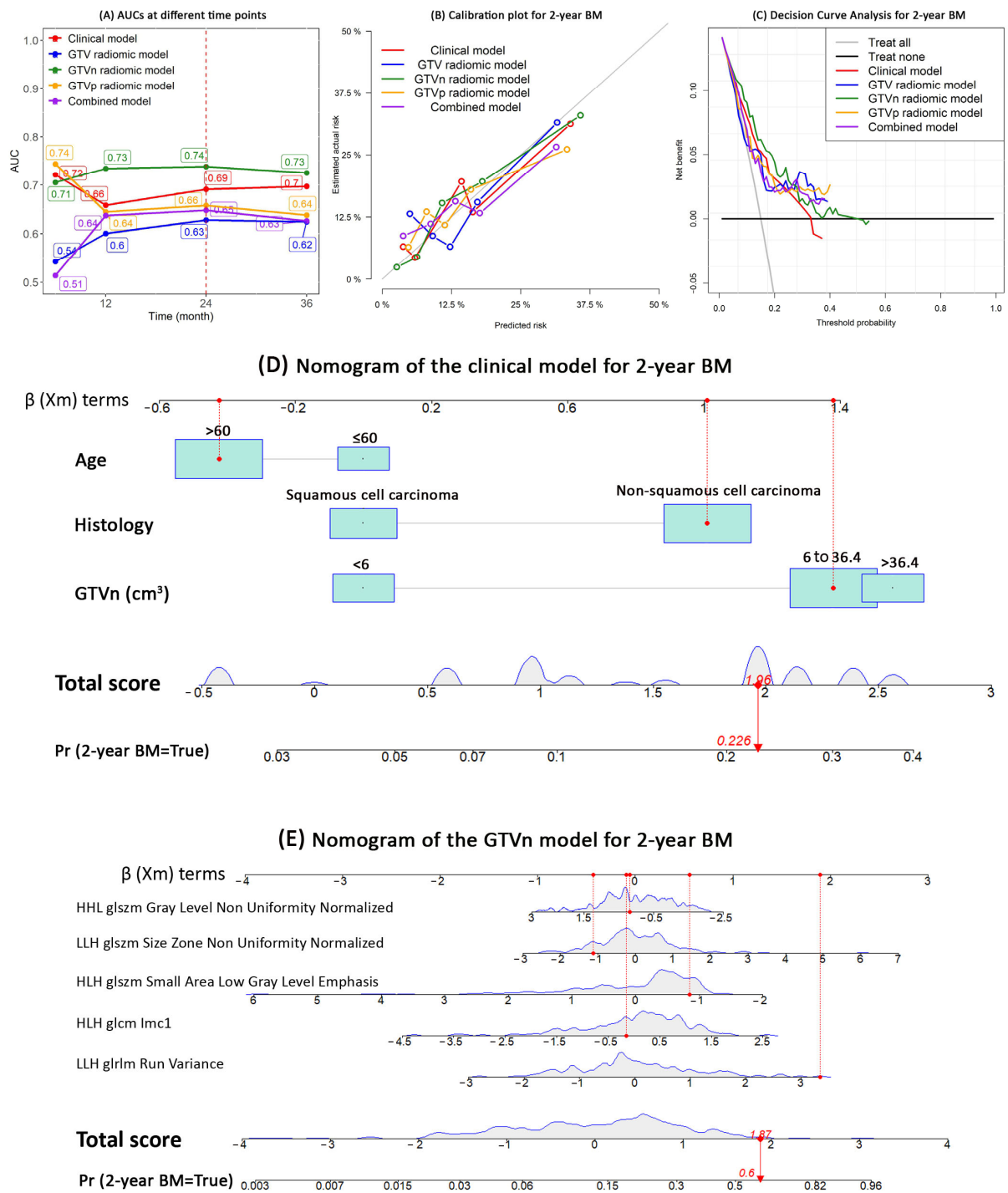


**Figure 3.** Models performance and nomogram. This figure shows the performance of the competing risk models for BM development in patients with radically treated stage III NSCLC (clinical, GTV, GTVn, GTVp, and combined models): (A) AUC; (B) Calibration plots; (C) Net—benefit decision curves; (D) nomogram of the clinical model; (E) nomogram of the GTVn radiomics model. *Abbreviations:* AUC, area under the receiver operating characteristic curves; BM, brain metastases; GTV, gross tumor volume; GTVp, GTV of the primary tumor; GTVn, GTV of the involved lymph nodes; NSCLC, non—small cell lung cancer.

**Table 3.** Model Performance at 24-months.

Models	AUC (95% CI)	Sensitivity	Specificity	PPV	NPV	Accuracy
Clinical	0.69 (0.66–0.82)	59%	77%	33%	91%	74%
GTV	0.63 (0.57–0.77)	65%	67%	27%	91%	67%
GTVn	0.74 (0.71–0.86)	84%	61%	29%	95%	65%
GTVp	0.66 (0.62–0.81)	54%	80%	34%	90%	76%
Combined	0.65 (0.60–0.78)	70%	60%	25%	91%	62%

*Abbreviations:* GTV, gross tumor volume; GTVp, gross tumor volume—primary lung tumor; GTVn, gross tumor volume—metastatic lymph nodes; AUC, area under the curve; CI, confidence interval; PPV, positive predictive value; NPV, negative predictive value.

### 3.3. OS, PFS

The above factors and radiomics features were checked for their impact on PFS and OS. A larger GTVn was significantly associated with decreased OS (median IQR: HR 1.49, 95% CI 1.01–2.21,  $p = 0.045$ ; upper IQR: HR 2.32, 95% CI 1.50–3.59,  $p < 0.001$ ) and PFS (median IQR: HR 1.93, 95% CI 1.30–2.85,  $p = 0.001$ ; upper IQR: HR 2.08, 95% CI 1.31–3.30,  $p = 0.002$ ). Patients with non-squamous carcinoma were at higher risk for progression (HR 1.35, 95% CI 1.00–1.83,  $p = 0.05$ ), but no significant association with OS was found. Age was not significantly correlated with OS or PFS (Tables A1 and A2).

All the five GTV radiomics features were not correlated with OS. HLH first-order Median of the GTV was correlated with PFS (HR 0.87, 95% CI 0.78–0.98,  $p = 0.02$ ) (Tables A1 and A2).

LLH glrlm Run Variance (HR 1.20, 95% CI 1.04–1.39,  $p = 0.016$ ) and HLH glszm Small Area Low Grey Level Emphasis of the GTVn (HR 0.78, 95% CI 0.63–0.97,  $p = 0.026$ ) was associated with OS, but not PFS (Tables A2 and A3).

LLL glcm Imc1 of GTVp was correlated with OS (HR 1.32, 95% CI 1.09–1.60,  $p = 0.005$ ) and PFS (HR 1.38, 95% CI 1.15–1.65,  $p = 0.001$ ). HLH glszm Grey Level Non Uniformity of GTVp was correlated with OS (HR 1.17, 95% CI 1.00–1.37,  $p = 0.047$ ) but not PFS. LLH glcm Cluster Shade of GTVp was correlated with PFS (HR 1.16, 95% CI 1.02–1.33,  $p = 0.026$ ) but not OS. (Tables A2 and A3).

The combined model showed that HLH glszm Grey Level Non Uniformity of GTVp was correlated with OS (HR 1.17, 95% CI 1.02–1.33,  $p = 0.023$ ) but not PFS. GTVn was associated with PFS (median IQR: HR 1.63, 95% CI 0.99–2.69,  $p = 0.054$ ; upper IQR: HR 2.37, 95% CI 1.28–4.38,  $p = 0.006$ ) but not OS (Tables A2 and A3).

## 4. Discussion

Although it has been reported that the GTV volume is associated with OS and PFS, the association of the GTV volume and the subsequent risk of BM development is unclear in patients with radically treated stage III NSCLC. Our study indicated that a larger GTVn was a risk factor for BM, OS, and PFS in patients with stage III NSCLC, but GTV and GTVp were not significantly associated with BM. In contrast, Ji et al. reported that GTV was not a significant risk factor for BM ( $p = 0.687$ ) [10]. A possible explanation could be that they analyzed the BM risk factors using Cox regression, which does not consider the competing event of death. Additionally, GTVp and GTVn were not specified. To the best of our knowledge, this is the first work reporting that GTVn is associated with subsequent BM development, while GTVp and GTV are not. The finding that lymph nodes involvement is more prognostic than the primary tumor volume warrants validation in further studies. A biological explanation could be that lung cancer cells are already more aggressive when migrating to lymph nodes and that the volume of GTVn correlates with the aggressiveness.

Interestingly, colleagues in Denmark investigated GTVp and GTVn for the first failure site in patients with locally advanced NSCLC. They found that neither GTVp nor GTVn was significantly correlated with first failure site (either locoregional failure or distant metastases) [30]. In this study, the main idea of separating GTVn from GTVp was similar to ours. However, patients with stage I-II or stage IV (20.5%) were also included, and

they only explored the associations with the first failure site without specifying BM or metastases to other organs. We focused on BM, regardless of whether the brain was the first site of failure and we also evaluated the association with PFS and OS. This approach is more inclusive and therefore of greater clinical practice value, as patients can still develop BM after extracranial progression.

In line with other studies [2–4,31], we also found that higher age ( $p = 0.05$ ) and squamous cell carcinoma ( $p = 0.009$ ) were independent protective factors for developing BM, while smoking history, thoracic radiotherapy dose, and the use of adjuvant durvalumab were not significantly associated with the development of BM ( $p > 0.05$ ). The latter was in contrast to the PACIFIC trial, in which the percentage of patients with BM halved in the durvalumab arm compared with placebo (31/476 [6.5%] vs. 28/237 [11.8%],  $p = 0.015$ ) [32]. A possible explanation could be that in the PACIFIC study only fit patients without disease progression after CCRT were selected [33], while we included NSCLC patients who had stage III at the initial diagnosis, patients who progressed after CCRT were not excluded. In addition, in the PACIFIC trial, brain MRI was not required (brain CT was allowed) and PET-CT was not mandatory, while in this current study, only patients who underwent baseline PET-CT and brain MRI to fully stage and exclude occult BM were included.

As far as we are aware, this is the first study which found that the GTVn radiomics model performed better than the clinical, GTVp radiomics, GTV radiomics, and combined model, with the highest AUC (0.74), sensitivity (84%), and NPV (95%). Consistent with earlier studies, the GTVp radiomics model was not as good as the clinical model [18]. Generally, a high sensitivity leads to a better ability of ruling a disease out, and a high specificity leads to a better ability of ruling in a disease [34]. As our aim of this study is to identify patients who are at higher risk of developing BM, it is better in ruling out BM (higher sensitivity) than ruling in BM, which indicates that management to prevent or detect BM (such as prophylactic cranial irradiation [PCI] and regular brain MRI surveillance) is needed for these patients. Therefore, although the GTVp radiomics model had a better specificity, we considered the GTVn radiomics model as a better one. Furthermore, an NPV of 95% is very good. Although the PPV and overall accuracy of the GTVn model were not great, the model may still be very valuable in clinical practice, as it can predict with a high likelihood that a patient will not develop BM and hence should not be considered for PCI (currently only within a clinical trial) nor for brain image follow-up. In addition, the specificity and sensitivity do not change when the incidence/prevalence changes, while the PPV and NPV are dependent on the prevalence/incidence of the outcome [34]. The relatively low PPV of all the models is mainly because of the relatively low incidence of BM (14.5% at 2 years) in this cohort, which was probably due to better staging (PET-CT and MRI were performed at diagnosis of stage III NSCLC). Therefore, the GTVp and GTVn should be separately delineated and analyzed in clinical practice and related studies.

Our results showed that wavelet features were the most prominent class associated with BM development as well as OS and PFS, independently from the region of interest of choice (GTV, GTVp, GTVn). Wavelet features decompose the original CT scan into a frequency space (like an “MR-like” image) and they are able to quantify granular textures based on the differences among harder and softer tissues. Our results showed that a combination of high-pass (HLH) and low-pass filtered (LLH) wavelet features are capable of quantifying tumor heterogeneity, which is a potential surrogate for a higher tumor aggressiveness. Although in the literature there is a lack of understanding about the biological meaning of radiomic features, our results suggest that tumors (and more specifically lymph nodes) that have more enhanced textures (GLSZM features) are more likely to spread to the brain, probably suggesting a higher proliferation of aggressive cells. Additionally, there are few studies that focused on extracting the radiomic features from both the GTVp and GTVn. However, previous radiomic studies [35,36] have shown that for the prediction of distant metastases it is better to focus on a larger region than just the GTVp, the so-called peri-tumoral ring.

In addition, we provided nomograms for the clinical model and the GTVn radiomics model, together with the codes for extracting radiomics features from GTVs on the planning CT scan, which clinicians and researchers could use for conducting future studies.

Strengths of this study are the relatively large dataset, the gold standard staging (baseline PET-CT and brain MRI), the administration of radical treatment to every patient, the inclusion of immunotherapy data in a real-world setting, and the long follow-up. All GTVs were rigorously contoured and evaluated by a team of specialists in lung cancer radiotherapy. Planning CTs were homogeneous regarding the scanning protocol. One limitation lies in the fact that we used the planning CT rather than the staging CT before anti-tumor treatment. In CCRT, most patients already had received one chemotherapy administration before having the planning CT. In SCRT, only patients with a reasonable performance status and without progression after chemotherapy were sent for thoracic radiotherapy. One can question the necessity of predicting the risk of BM in patients intended to undergo SCRT but not eligible (progression, poor PS) to undergo thoracic radiotherapy. On the other hand, the use of expertly contoured GTVs is reliable as well as convenient because no additional contouring is necessary, and therefore extracting radiomics features from GTVs is feasible in clinical application for all patients with a radiotherapy treatment plan. Another limitation is the lack of external validation. To overcome this limitation, we performed bootstrapping 1000 times and LASSO regression to develop the radiomics models. Our results can be further tested in future external validation studies (evaluating our model on a separate dataset, TRIPOD type 4 studies), or further confirmed using the same methods with a larger sample size training dataset and an independent validation dataset (TRIPOD type 3 studies) [29].

## 5. Conclusions

To our knowledge, this is the first study that demonstrates the prognostic value of the GTVn volume on BM development in patients with stage III NSCLC. Younger patients and those with non-squamous cell carcinoma are at higher risk of developing BM. Radiomics features of GTVn have greater prognostic value than GTVp and GTV for BM development. Therefore, the GTVp and GTVn will be contoured and analyzed separately in clinical practice and future studies.

**Author Contributions:** Conception and design: H.Z., D.K.M.D.R. and L.E.L.H.; Provision of study materials or patients: H.Z., J.H.R.J.D., V.E.M.v.K.-v.d.B., C.P., F.C. and L.E.L.H. Collection and assembly of data: H.Z., Y.C.P.W. Data analysis and interpretation: H.Z., F.T., D.K.M.D.R., L.B., L.E.L.H. and A.T. All authors have read and agreed to the published version of the manuscript.

**Funding:** This research was supported by the following grant: China Scholarship Council (Grant No.: CSC 201909370087).

**Institutional Review Board Statement:** This study was conducted in accordance with the Helsinki Declaration of the World Medical Association and approved by the institutional review board of Maastrro (W 22 01 00001, approved on 19 January 2021) and Institutional Ethics Committee of University Hospital of Udine (protocol 2022-OS-121, approved on 12 October 2022).

**Informed Consent Statement:** Informed consent from individuals for the use of their medical data was waived because no additional interventions were performed.

**Data Availability Statement:** Data sharing is possible upon reasonable request to the corresponding author and with the approval of institutional review board IRBs. The details of the radiomics source code are published on a public repository (<https://github.com/Maastrro-CDS-Imaging-Group/GTVNSCLC>; accessed on 27 March 2023).

**Acknowledgments:** We sincerely thank all the radiation oncologists for their contributions to delineate GTVs and the ICT departments of each center for logistic supports.

**Conflicts of Interest:** The authors declare no conflict of interest.

## Appendix A

**Table A1.** TRIPOD Checklist: Prediction Model Development.

Section/Topic	Item	Checklist Item	Page
<b>Title and abstract</b>			
Title	1	Identify the study as developing and/or validating a multivariable prediction model, the target population, and the outcome to be predicted.	1
Abstract	2	Provide a summary of objectives, study design, setting, participants, sample size, predictors, outcome, statistical analysis, results, and conclusions.	1
<b>Introduction</b>			
Background and objectives	3a	Explain the medical context (including whether diagnostic or prognostic) and rationale for developing or validating the multivariable prediction model, including references to existing models.	2–3
	3b	Specify the objectives, including whether the study describes the development or validation of the model or both.	3
<b>Methods</b>			
Source of data	4a	Describe the study design or source of data (e.g., randomized trial, cohort, or registry data), separately for the development and validation datasets, if applicable.	3
	4b	Specify the key study dates, including start of accrual; end of accrual; and, if applicable, end of follow-up.	3
Participants	5a	Specify key elements of the study setting (e.g., primary care, secondary care, general population) including number and location of centres.	3
	5b	Describe eligibility criteria for participants.	3
	5c	Give details of treatments received, if relevant.	3
Outcome	6a	Clearly define the outcome that is predicted by the prediction model, including how and when assessed.	5
	6b	Report any actions to blind assessment of the outcome to be predicted.	NA
Predictors	7a	Clearly define all predictors used in developing or validating the multivariable prediction model, including how and when they were measured.	3–5
	7b	Report any actions to blind assessment of predictors for the outcome and other predictors.	NA
Sample size	8	Explain how the study size was arrived at.	3
Missing data	9	Describe how missing data were handled (e.g., complete-case analysis, single imputation, multiple imputation) with details of any imputation method.	5
Statistical analysis methods	10a	Describe how predictors were handled in the analyses.	5
	10b	Specify type of model, all model-building procedures (including any predictor selection), and method for internal validation.	5–6, Figure 2.5
	10d	Specify all measures used to assess model performance and, if relevant, to compare multiple models.	6
Risk groups	11	Provide details on how risk groups were created, if done.	NA
<b>Results</b>			
Participants	13a	Describe the flow of participants through the study, including the number of participants with and without the outcome and, if applicable, a summary of the follow-up time. A diagram may be helpful.	6, Figure 2
	13b	Describe the characteristics of the participants (basic demographics, clinical features, available predictors), including the number of participants with missing data for predictors and outcome.	6, Table 1

Table A1. Cont.

Section/Topic	Item	Checklist Item	Page
Model development	14a	Specify the number of participants and outcome events in each analysis.	6–7
	14b	If done, report the unadjusted association between each candidate predictor and outcome.	NA
Model specification	15a	Present the full prediction model to allow predictions for individuals (i.e., all regression coefficients, and model intercept or baseline survival at a given time point).	6–7. Tables 2 and 3
	15b	Explain how to use the prediction model.	7, Figure 3
Model performance	16	Report performance measures (with CIs) for the prediction model.	7
<b>Discussion</b>			
Limitations	18	Discuss any limitations of the study (such as nonrepresentative sample, few events per predictor, missing data).	10–11
Interpretation	19b	Give an overall interpretation of the results, considering objectives, limitations, and results from similar studies, and other relevant evidence.	8–11
Implications	20	Discuss the potential clinical use of the model and implications for future research.	10
<b>Other information</b>			
Supplementary information	21	Provide information about the availability of supplementary resources, such as study protocol, Web calculator, and datasets.	5
Funding	22	Give the source of funding and the role of the funders for the present study.	Title page

Table A2. Overall survival Cox models.

	HR	95% CI	<i>p</i>
<b>Clinical model</b> ( <i>n</i> = 310, 176 death)			
Age (>60 vs. ≤60)	1.44	0.98–2.11	0.066
Histology (Non-Squamous vs. squamous)	1.08	0.79–1.46	0.645
GTVn (cm <sup>3</sup> )			
<6		[Reference]	
6–36.4	1.49	1.01–2.21	<b>0.045</b>
>36.4	2.32	1.50–3.59	<b>&lt;0.001</b>
<b>GTV radiomic model</b> ( <i>n</i> = 282, 168 death)			
HLH firstorder Median	1.00	0.91–1.11	0.977
HLH glcm Imc1	1.08	0.91–1.28	0.392
Original firstorder Skewness	0.95	0.81–1.12	0.55
Original glszm Zone Entropy	1.19	0.98–1.43	0.081
HHH glszm Small Area Emphasis	1.01	0.85–1.18	0.95
<b>GTVn radiomic model</b> ( <i>n</i> = 254, 158 death)			
LLH glrlm Run Variance	1.20	1.04–1.39	<b>0.016</b>
HLH glcm Imc1	1.01	0.86–1.20	0.873
HLH glszm Small Area Low Grey Level Emphasis	0.78	0.63–0.97	<b>0.026</b>
LLH glszm Size Zone Non Uniformity Normalized	1.03	0.88–1.20	0.717
HHL glszm Grey Level Non Uniformity Normalized	1.04	0.88–1.23	0.648
<b>GTVp radiomic model</b> ( <i>n</i> = 260, 153 death)			
LHH glszm Small Area Low Grey Level Emphasis	1.15	0.96–1.39	0.132
LLH glcm Cluster Shade	1.02	0.88–1.18	0.83
HLH glszm Grey Level Non Uniformity	1.17	1.00–1.37	<b>0.047</b>
HLL firstorder Root Mean Squared	0.97	0.79–1.20	0.797
LLL glcm Imc1	1.32	1.09–1.60	<b>0.005</b>

**Table A2.** *Cont.*

	HR	95% CI	<i>p</i>
<b>Combined model</b> ( <i>n</i> = 231, 142 death)			
GTVn (cm <sup>3</sup> )			
<6		[Reference]	
6–36.4	1.10	0.67–1.78	0.716
>36.4	1.70	0.94–3.09	0.081
GTV HLH glcm Imc1	1.05	0.85–1.29	0.655
GTVn LLH glrlm Run Variance	1.12	0.93–1.35	0.23
GTVp HLH glszm Grey Level Non Uniformity	1.17	1.02–1.33	<b>0.023</b>

*Abbreviations:* CI, confidence interval; GTV, gross tumor volume; GTVp, gross tumor volume-primary lung tumor; GTVn, gross tumor volume-metastatic lymph nodes; HR, hazard ratio.

**Table A3.** Progression-free survival Cox models.

	HR	95% CI	<i>p</i>
<b>Clinical model</b> ( <i>n</i> = 310, 183 progression)			
Age (>60 vs. ≤60)	1.12	0.78–1.63	0.537
Histology (Non—Squamous vs. squamous)	1.35	1.00–1.83	0.054
GTVn (cm <sup>3</sup> )			
<6		[Reference]	
6–36.4	1.93	1.30–2.85	<b>0.001</b>
>36.4	2.08	1.31–3.30	<b>0.002</b>
<b>GTV radiomic model</b> ( <i>n</i> = 282, 167 progression)			
HLH firstorder Median	0.87	0.78–0.98	<b>0.02</b>
HLH glcm Imc1	1.06	0.90–1.25	0.51
Original firstorder Skewness	1.07	0.89–1.27	0.494
Original glszm Zone Entropy	1.02	0.86–1.22	0.787
HHH glszm Small Area Emphasis	1.05	0.90–1.23	0.531
<b>GTVn radiomic model</b> ( <i>n</i> = 254, 156 progression)			
LLH glrlm Run Variance	1.03	0.87–1.23	0.733
HLH glcm Imc1	1.12	0.94–1.32	0.204
HLH glszm Small Area Low Grey Level Emphasis	0.84	0.69–1.01	0.065
LLH glszm Size Zone Non Uniformity	1.14	0.97–1.33	0.105
Normalized			
HHL glszm Grey Level Non Uniformity	1.01	0.85–1.19	0.944
Normalized			
<b>GTVp radiomic model</b> ( <i>n</i> = 260, 157 progression)			
LHH glszm Small Area Low Grey Level Emphasis	1.17	0.99–1.38	0.06
LLH glcm Cluster Shade	1.16	1.02–1.33	<b>0.026</b>
HLH glszm Grey Level Non Uniformity	1.16	0.96–1.40	0.121
HLL firstorder Root Mean Squared	0.93	0.77–1.13	0.453
LLL glcm Imc1	1.38	1.15–1.65	<b>0.001</b>
<b>Combined model</b> ( <i>n</i> = 231, 145 progression)			
GTVn (cm <sup>3</sup> )			
<6		[Reference]	
6–36.4	1.63	0.99–2.69	0.054
>36.4	2.37	1.28–4.38	<b>0.006</b>
GTV HLH glcm Imc1	1.06	0.86–1.30	0.593
GTVn LLH glrlm Run Variance	0.96	0.78–1.18	0.679
GTVp HLH glszm Grey Level Non Uniformity	1.13	0.98–1.31	0.1

*Abbreviations:* CI, confidence interval; GTV, gross tumor volume; GTVp, gross tumor volume-primary lung tumor; GTVn, gross tumor volume-metastatic lymph nodes; HR, hazard ratio.

## References

1. De Ruyscher, D.; Dingemans, A.C.; Praag, J.; Belderbos, J.; Tissing-Tan, C.; Herder, J.; Haitjema, T.; Ubbels, F.; Lagerwaard, F.; El Sharouni, S.Y.; et al. Prophylactic Cranial Irradiation Versus Observation in Radically Treated Stage III Non-Small-Cell Lung Cancer: A Randomized Phase III NVALT-11/DLCRG-02 Study. *J. Clin. Oncol. Off. J. Am. Soc. Clin. Oncol.* **2018**, *36*, 2366–2377. [[CrossRef](#)] [[PubMed](#)]
2. Chen, S.; Hua, X.; Jia, J.; Wu, Y.; Wei, S.; Xu, L.; Han, S.; Zhang, H.; Zhu, X. Risk factors for brain metastases in patients with non-small cell lung cancer: A meta-analysis of 43 studies. *Ann. Palliat. Med.* **2021**, *10*, 3657–3672. [[CrossRef](#)] [[PubMed](#)]
3. An, N.; Jing, W.; Wang, H.; Li, J.; Liu, Y.; Yu, J.; Zhu, H. Risk factors for brain metastases in patients with non-small-cell lung cancer. *Cancer Med.* **2018**, *7*, 6357–6364. [[CrossRef](#)] [[PubMed](#)]
4. Sun, D.S.; Hu, L.K.; Cai, Y.; Li, X.M.; Ye, L.; Hou, H.Y.; Wang, C.H.; Jiang, Y.H. A systematic review of risk factors for brain metastases and value of prophylactic cranial irradiation in non-small cell lung cancer. *Asian Pac. J. Cancer Prev.* **2014**, *15*, 1233–1239. [[CrossRef](#)]
5. Soliman, M.; Yaromina, A.; Appold, S.; Zips, D.; Reiffenstuhel, C.; Schreiber, A.; Thames, H.D.; Krause, M.; Baumann, M. GTV differentially impacts locoregional control of non-small cell lung cancer (NSCLC) after different fractionation schedules: Subgroup analysis of the prospective randomized CHARTWEL trial. *Radiother. Oncol.* **2013**, *106*, 299–304. [[CrossRef](#)]
6. Chen, N.B.; Li, Q.W.; Zhu, Z.F.; Wang, Y.M.; Cheng, Z.J.; Hui, Z.G.; Guo, S.P.; He, H.Q.; Wang, B.; Huang, X.Y.; et al. Developing and validating an integrated gross tumor volume (GTV)-TNM stratification system for supplementing unresectable locally advanced non-small cell lung cancer treated with concurrent chemoradiotherapy. *Radiat. Oncol. (Lond. Engl.)* **2020**, *15*, 260. [[CrossRef](#)]
7. Dehing-Oberije, C.; Aerts, H.; Yu, S.; De Ruyscher, D.; Menheere, P.; Hilvo, M.; van der Weide, H.; Rao, B.; Lambin, P. Development and validation of a prognostic model using blood biomarker information for prediction of survival of non-small-cell lung cancer patients treated with combined chemotherapy and radiation or radiotherapy alone (NCT00181519, NCT00573040, and NCT00572325). *Int. J. Radiat. Oncol. Biol. Phys.* **2011**, *81*, 360–368.
8. Dehing-Oberije, C.; Yu, S.; De Ruyscher, D.; Meersschout, S.; Van Beek, K.; Lievens, Y.; Van Meerbeeck, J.; De Neve, W.; Rao, B.; van der Weide, H.; et al. Development and external validation of prognostic model for 2-year survival of non-small-cell lung cancer patients treated with chemoradiotherapy. *Int. J. Radiat. Oncol. Biol. Phys.* **2009**, *74*, 355–362. [[CrossRef](#)]
9. Van Laar, M.; van Amsterdam, W.A.C.; van Lindert, A.S.R.; de Jong, P.A.; Verhoeff, J.J.C. Prognostic factors for overall survival of stage III non-small cell lung cancer patients on computed tomography: A systematic review and meta-analysis. *Radiother. Oncol.* **2020**, *151*, 152–175. [[CrossRef](#)]
10. Ji, Z.; Bi, N.; Wang, J.; Hui, Z.; Xiao, Z.; Feng, Q.; Zhou, Z.; Chen, D.; Lv, J.; Liang, J.; et al. Risk factors for brain metastases in locally advanced non-small cell lung cancer with definitive chest radiation. *Int. J. Radiat. Oncol. Biol. Phys.* **2014**, *89*, 330–337. [[CrossRef](#)]
11. Levy, A.; Le Péchoux, C.; Mistry, H.; Martel-Lafay, I.; Bezjak, A.; Lerouge, D.; Padovani, L.; Taylor, P.; Faivre-Finn, C. Prophylactic Cranial Irradiation for Limited-Stage Small-Cell Lung Cancer Patients: Secondary Findings from the Prospective Randomized Phase 3 CONVERT Trial. *J. Thorac. Oncol.* **2019**, *14*, 294–297. [[CrossRef](#)]
12. Zhang, J.; Jin, J.; Ai, Y.; Zhu, K.; Xiao, C.; Xie, C.; Jin, X. Computer Tomography Radiomics-Based Nomogram in the Survival Prediction for Brain Metastases from Non-Small Cell Lung Cancer Underwent Whole Brain Radiotherapy. *Front. Oncol.* **2020**, *10*, 610691. [[CrossRef](#)]
13. Zhao, S.; Hou, D.; Zheng, X.; Song, W.; Liu, X.; Wang, S.; Zhou, L.; Tao, X.; Lv, L.; Sun, Q.; et al. MRI radiomic signature predicts intracranial progression-free survival in patients with brain metastases of ALK-positive non-small cell lung cancer. *Transl. Lung Cancer Res.* **2021**, *10*, 368–380. [[CrossRef](#)]
14. Paget, S. The distribution of secondary growths in cancer of the breast. *Lancet* **1889**, *1*, 99–101. [[CrossRef](#)]
15. Chen, A.; Lu, L.; Pu, X.; Yu, T.; Yang, H.; Schwartz, L.H.; Zhao, B. CT-Based Radiomics Model for Predicting Brain Metastasis in Category T1 Lung Adenocarcinoma. *AJR Am. J. Roentgenol.* **2019**, *213*, 134–139. [[CrossRef](#)]
16. Xu, X.; Huang, L.; Chen, J.; Wen, J.; Liu, D.; Cao, J.; Wang, J.; Fan, M. Application of radiomics signature captured from pretreatment thoracic CT to predict brain metastases in stage III/IV ALK-positive non-small cell lung cancer patients. *J. Thorac. Dis.* **2019**, *11*, 4516–4528. [[CrossRef](#)]
17. Sun, F.; Chen, Y.; Chen, X.; Sun, X.; Xing, L. CT-based radiomics for predicting brain metastases as the first failure in patients with curatively resected locally advanced non-small cell lung cancer. *Eur. J. Radiol.* **2021**, *134*, 109411. [[CrossRef](#)]
18. Keek, S.A.; Kayan, E.; Chatterjee, A.; Belderbos, J.S.A.; Bootsma, G.; van den Borne, B.; Dingemans, A.C.; Gietema, H.A.; Groen, H.J.M.; Herder, J.; et al. Investigation of the added value of CT-based radiomics in predicting the development of brain metastases in patients with radically treated stage III NSCLC. *Ther. Adv. Med. Oncol.* **2022**, *14*, 116605. [[CrossRef](#)]
19. Wang, H.; Chen, Y.Z.; Li, W.H.; Han, Y.; Li, Q.; Ye, Z. Pretreatment Thoracic CT Radiomic Features to Predict Brain Metastases in Patients With ALK-Rearranged Non-Small Cell Lung Cancer. *Front. Genet.* **2022**, *13*, 772090. [[CrossRef](#)]
20. Goldstraw, P.; Crowley, J.; Chansky, K.; Giroux, D.J.; Groome, P.A.; Rami-Porta, R.; Postmus, P.E.; Rusch, V.; Sobin, L. The IASLC Lung Cancer Staging Project: Proposals for the revision of the TNM stage groupings in the forthcoming (seventh) edition of the TNM Classification of malignant tumours. *J. Thorac. Oncol.* **2007**, *2*, 706–714. [[CrossRef](#)]

21. Van Diessen, J.; De Ruyscher, D.; Sonke, J.J.; Damen, E.; Sikorska, K.; Reymen, B.; van Elmpt, W.; Westman, G.; Persson, G.F.; Dieleman, E.; et al. The acute and late toxicity results of a randomized phase II dose-escalation trial in non-small cell lung cancer (PET-boost trial). *Radiother. Oncol.* **2019**, *131*, 166–173. [[CrossRef](#)] [[PubMed](#)]
22. Peters, S.; Felip, E.; Dafni, U.; Tufman, A.; Guckenberger, M.; Álvarez, R.; Nadal, E.; Becker, A.; Veer, H.; Pless, M.; et al. Progression-Free and Overall Survival for Concurrent Nivolumab with Standard Concurrent Chemoradiotherapy in Locally Advanced Stage IIIA-B NSCLC: Results From the European Thoracic Oncology Platform NICOLAS Phase II Trial (European Thoracic Oncology Platform 6-14). *J. Thorac. Oncol.* **2021**, *16*, 278–288. [[PubMed](#)]
23. Nestle, U.; Le Pechoux, C.; De Ruyscher, D. Evolving target volume concepts in locally advanced non-small cell lung cancer. *Transl. Lung Cancer Res.* **2021**, *10*, 1999–2010. [[CrossRef](#)] [[PubMed](#)]
24. Gray, R.J. A class of K-sample tests for comparing the cumulative incidence of a competing risk. *Ann. Stat.* **1988**, *16*, 1141–1154. [[CrossRef](#)]
25. Fine, J.P.; Gray, R.J. A Proportional Hazards Model for the Subdistribution of a Competing Risk. *J. Am. Stat. Assoc.* **1999**, *94*, 496–509. [[CrossRef](#)]
26. Zhang, Z.; Wang, Z.; Yan, M.; Yu, J.; Dekker, A.; Zhao, L.; Wee, L. Radiomics and Dosiomics Signature From Whole Lung Predicts Radiation Pneumonitis: A Model Development Study With Prospective External Validation and Decision-curve Analysis. *Int. J. Radiat. Oncol. Biol. Phys.* **2023**, *115*, 746–758. [[CrossRef](#)]
27. Compter, I.; Verduin, M.; Shi, Z.; Woodruff, H.C.; Smeenk, R.J.; Rozema, T.; Leijenaar, R.T.H.; Monshouwer, R.; Eekers, D.B.P.; Hoeben, A.; et al. Deciphering the glioblastoma phenotype by computed tomography radiomics. *Radiother. Oncol.* **2021**, *160*, 132–139. [[CrossRef](#)]
28. Tohidinezhad, F.; Bontempi, D.; Zhang, Z.; Dingemans, A.M.; Aerts, J.; Bootsma, G.; Vansteenkiste, J.; Hashemi, S.; Smit, E.; Gietema, H.; et al. Computed tomography-based radiomics for the differential diagnosis of pneumonitis in stage IV non-small cell lung cancer patients treated with immune checkpoint inhibitors. *Eur. J. Cancer* **2023**, *183*, 142–151. [[CrossRef](#)]
29. Collins, G.S.; Reitsma, J.B.; Altman, D.G.; Moons, K.G. Transparent Reporting of a multivariable prediction model for Individual Prognosis or Diagnosis (TRIPOD): The TRIPOD Statement. *Br. J. Surg.* **2015**, *102*, 148–158. [[CrossRef](#)]
30. Lacoppidan, T.; Vogelius, I.R.; Pøhl, M.; Strange, M.; Persson, G.F.; Nygård, L. An investigative expansion of a competing risk model for first failure site in locally advanced non-small cell lung cancer. *Acta Oncol.* **2019**, *58*, 1386–1392. [[CrossRef](#)]
31. Zeng, H.; Zheng, D.; Witlox, W.J.A.; Levy, A.; Traverso, A.; Kong, F.S.; Houben, R.; De Ruyscher, D.K.M.; Hendriks, L.E.L. Risk Factors for Brain Metastases in Patients with Small Cell Lung Cancer: A Systematic Review and Meta-Analysis. *Front. Oncol.* **2022**, *12*, 889161. [[CrossRef](#)]
32. Spigel, D.R.; Faivre-Finn, C.; Gray, J.E.; Vicente, D.; Planchard, D.; Paz-Ares, L.; Vansteenkiste, J.F.; Garassino, M.C.; Hui, R.; Quantin, X.; et al. Five-Year Survival Outcomes from the PACIFIC Trial: Durvalumab After Chemoradiotherapy in Stage III Non-Small-Cell Lung Cancer. *J. Clin. Oncol. Off. J. Am. Soc. Clin. Oncol.* **2022**, *40*, 1301–1311. [[CrossRef](#)]
33. Antonia, S.J.; Villegas, A.; Daniel, D.; Vicente, D.; Murakami, S.; Hui, R.; Yokoi, T.; Chiappori, A.; Lee, K.H.; de Wit, M.; et al. Durvalumab after Chemoradiotherapy in Stage III Non-Small-Cell Lung Cancer. *N. Engl. J. Med.* **2017**, *377*, 1919–1929. [[CrossRef](#)]
34. Loong, T.W. Understanding sensitivity and specificity with the right side of the brain. *BMJ* **2003**, *327*, 716–719. [[CrossRef](#)]
35. Takehana, K.; Sakamoto, R.; Fujimoto, K.; Matsuo, Y.; Nakajima, N.; Yoshizawa, A.; Menju, T.; Nakamura, M.; Yamada, R.; Mizowaki, T.; et al. Peritumoral radiomics features on preoperative thin-slice CT images can predict the spread through air spaces of lung adenocarcinoma. *Sci. Rep.* **2022**, *12*, 10323. [[CrossRef](#)]
36. Pérez-Morales, J.; Tunali, I.; Stringfield, O.; Eschrich, S.A.; Balagurunathan, Y.; Gillies, R.J.; Schabath, M.B. Peritumoral and intratumoral radiomics features predict survival outcomes among patients diagnosed in lung cancer screening. *Sci. Rep.* **2020**, *10*, 10528. [[CrossRef](#)]

**Disclaimer/Publisher’s Note:** The statements, opinions and data contained in all publications are solely those of the individual author(s) and contributor(s) and not of MDPI and/or the editor(s). MDPI and/or the editor(s) disclaim responsibility for any injury to people or property resulting from any ideas, methods, instructions or products referred to in the content.